

Effects of Short-Chain Chlorinated Paraffins Exposure on the Viability and Metabolism of Human Hepatoma HepG2 Cells

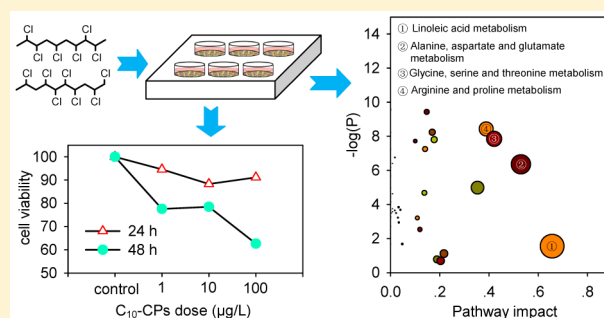
Ningbo Geng,^{†,‡} Haijun Zhang,^{*,†} Baoqin Zhang,[†] Ping Wu,[†] Feidi Wang,^{†,‡} Zhengkun Yu,[†] and Jiping Chen^{*,†}

[†]Dalian Institute of Chemical Physics, Chinese Academy of Sciences, Dalian, 116023, China

[‡]Graduate School of Chinese Academy of Science, Beijing 100049, China

Supporting Information

ABSTRACT: Short-chain chlorinated paraffins (SCCPs) have attracted considerable attention for their characteristic of persistent organic pollutants. However, very limited information is available for their toxic effects at environmentally relevant doses, limiting the evaluation of their health risks. In this study, cell viability assay and targeted metabolomic approach was used to evaluate the environmental dose (<100 $\mu\text{g/L}$) effect of SCCPs on HepG2 cells. Cell viability was found to be decreased with increases in exposure dose of SCCPs. Exposure for 48 h to C_{10} -CPs resulted in a significant reduction in cell viability compared with 24 h, even at 1 $\mu\text{g/L}$. SCCPs exposure altered the intracellular redox status and caused significant metabolic disruptions. As a kind of peroxisome proliferator, SCCPs specifically stimulated the β -oxidation of unsaturated fatty acids and long-chain fatty acids. Meanwhile, SCCPs exposure disturbed glycolysis and amino acid metabolism, and led to the up-regulation of glutamate metabolism and urea cycle. The toxic effects of SCCPs might mainly involve the perturbation of energy production, protein biosynthesis, fatty acid metabolism, and ammonia recycling.



INTRODUCTION

Short-chain chlorinated paraffins (SCCPs, C_{10-13}) are a large and complex group of polychlorinated *n*-alkanes found ubiquitously in the environment.¹⁻⁴ They have been extensively used in metalworking fluids, paints, sealants, lubricant additives, flame retardants, and plasticizers as industrial additives.⁵ In 2009, SCCPs were reviewed as potential persistent organic pollutants (POPs) by the Stockholm Convention on POPs, concerning their persistence in the environment, long-range transport potential, liability to bioaccumulate, and high toxicity to aquatic organisms.^{3,6-8} However, whether the environmental SCCPs concentrations have resulted in “significant adverse human health effects” is still unknown, and evidence on the toxic action mechanisms of SCCPs is limited and controversial.^{9,10}

Assessment of the available data clearly indicates that SCCPs are of low acute toxicity in animals, although their carcinogenic toxicity has been demonstrated by a 2-year oral exposure study in F344/N rats and B6C3F1 mice.¹¹ The highest dose that can be given without showing an adverse effect (the no observed adverse effect level, NOAEL) is 10 mg/kg/day for rats.¹⁰ In subchronic toxicity studies on laboratory animals, SCCPs produce toxic effects on the kidney, liver, thyroid, and parathyroid glands.^{10,12} Studies in rats and mice exposed to SCCPs indicate that the liver damage is associated with peroxisome proliferation, whereas thyroid effects are correlated to altered thyroid hormone status and glucuronyl transferase

induction.¹² However, biological events involved in the cellular response are not completely elucidated. As a result, the underlying toxicity mechanisms of SCCPs remain in a “black box”.

Further studies on the toxic mechanisms of SCCPs are, therefore, in high demand. We hypothesize that SCCPs can induce oxidative stress, and hence alter the cellular metabolism and cell viability; meanwhile SCCPs can act as a peroxisome proliferator and specifically disturb lipid metabolism. To address above hypothesis, a metabolomic approach was applied to explore the metabolic response of human hepatoma HepG2 cells to SCCPs exposure. Metabolomics is a method of understanding metabolic regulation by studying small molecule metabolites. It can provide a “closer” glimpse into the phenotypic state of an organism because it is downstream of both proteomics and transcriptomics compared with that of functional genomic analysis.¹³ Metabolomics has been widely applied in biomarker discovery and toxic risk assessment in pharmacology and toxicology, as well as to reveal active pathways and signaling metabolites.^{14,15} In recent years, metabolomics has been applied for investigating metabolic changes in laboratory animals and cell lines exposed with high-

Received: May 16, 2014

Revised: February 2, 2015

Accepted: February 7, 2015

Published: February 7, 2015

toxicity organic pollutants, such as polychlorinated dibenzo-*p*-dioxins and furans,¹⁶ polycyclic aromatic hydrocarbons,¹⁷ polybrominated diphenyl ethers,¹⁸ perfluorooctanoic acid,¹⁹ and bisphenol A.²⁰ However, no metabolomic assessment for SCCPs toxicity has been conducted.

HepG2 cells can express a wide range of human liver-specific functions and have been widely used as a model for various omics studies concerning hepatotoxicity.^{21–23} The molecular expression and biological phenotypes of HepG2 cells have been extensively characterized, and thus, they can be used as metabolically relevant models for *in vitro* toxicology studies. In this study, the effects of SCCPs dose, chain length, and chlorine content on HepG2 cell viability were first performed to explore the potential toxicity of SCCPs, and then the oxidative stress induction, metabolic alteration and relevant metabolic enzyme activities were investigated. Furthermore, the physiological functions of metabolites that changed in response to SCCPs exposure were also considered. The obtained results were expected to provide a better understanding of the cellular disturbances induced by environmental dose-related SCCPs exposure and new toxicity evidence of SCCPs from a novel perspective at the molecular level.

EXPERIMENTAL SECTION

Chemicals and Materials. Phosphate-buffered saline (PBS), trypsin, fetal bovine serum (FBS), and Dulbecco's Modified Eagle's Medium (DMEM) were purchased from Gibco-BRL (Grand Island, NY, USA). 3-(4,5-Dimethylthiazol-2-yl)-2,5-diphenyl tetrazolium bromide (MTT; Amresco, Solon, OH, USA) was purchased from Sigma-Aldrich. Penicillin–streptomycin was obtained from Hyclone (Logan, UT, USA). Fatty acid, amino acid, lactic acid, urea, glucose, glycerol standards, and methyl *tert*-butyl ether (MTBE) were purchased from Aladdin Reagent Company. HPLC-grade ammonium acetate and formic acid were obtained from J&K Scientific (Beijing, China). HPLC-grade acetonitrile (ACN) and methanol were obtained from Fisher (Fair Lawn, NJ, USA). The water used in all experiments was ultrapure water from a Milli-Q system (Millipore, Billerica, MA, USA). A standard solution (mix-1) consisting of amino acids, lactic acid, urea, glucose, glycerol, and a standard solution consisting of fatty acids (mix-2) were used as the quality control (QC) samples for the polar and apolar fractions, respectively.

Cell Culture and Exposure Experiments. Human hepatoma HepG2 cells were cultured in DMEM supplemented with 10% FBS and 1% penicillin-streptomycin at 37 °C in a humidified atmosphere of 5% CO₂. The cells were rinsed with PBS, trypsinized, and then transferred onto culture plates in the logarithmic phase of growth. HepG2 cells seeded in a 96-well plate at a density of 2×10^4 cells/well were incubated for 24 or 48 h and then subjected to the assay of cell viability. HepG2 cells seeded in 6-well plates at 3×10^5 cells/well were cultured for 24 h and then submitted to the analysis of metabolites and the determination of oxidative stress markers and relevant metabolic enzyme activities, respectively.

After cell seeding and growing to 80% confluency, the SCCPs dissolved in DMSO were added into the cell culture medium. The final DMSO content in culture medium was 0.05% (v/v), and background control wells were treated with only 0.05% DMSO. HepG2 cells were exposed to the SCCPs congeners with varying concentrations (1, 10, and 100 μg/L) in culture medium, carbon chain lengths (C₁₀, C₁₁, C₁₂, and C₁₃-CPs; 100 μg/L) and chlorine contents (C₁₀-CPs, 100 μg/L;

L; chlorine content 40.4%, 57.9%, and 64.4%). The exposure doses of 1 and 10 μg/L are comparable with SCCPs concentrations in surface water²⁴ and human milk,²⁵ respectively. The SCCPs congeners with known carbon chain length and chlorine content used in this experiment were synthesized by chlorination of *n*-alkane in our laboratory.²⁶

Cell Viability Assay. Cell viability was tested using the MTT assay. When the SCCPs exposure experiment was finished, 20 μL of MTT (5 mg/mL, in PBS) was added directly to the culture medium, and then an additional 4-h incubation at 37 °C and 5% CO₂ was conducted. Violet crystals generated by viable cells were directly dissolved by 150 μL of DMSO and well-mixed for analysis. The optical density of the sample was quantified at a wavelength of 492 nm with a multiwell microplate reader (Tecan Infinite F50). The cell viability was calculated by setting the viability of the control cells as 100%.

Determination of Oxidative Stress Markers and Relevant Metabolic Enzyme Activities. To further explore the toxicity mechanisms of SCCPs, several oxidative stress markers, together with activities of some crucial metabolic enzymes regulating glycolytic pathway, glutamine metabolism, β-oxidation of fatty acid, and urea cycle, were determined. After exposure to C₁₃-SCCPs (Cl, 55.0%) with varying concentrations (0, 1, 10, and 100 μg/L) for 24 h, HepG2 cells were trypsinized, rinsed with PBS, and then resuspended in PBS for ultrasonic cell disruption. The supernatant was centrifuged and then subjected to the further analysis.

The specific assay kits (Nanjing Jiancheng Bioengineering Institute, China) were adopted to determine the level of reduced glutathione (GSH) and total protein (TP), the activities of superoxide dismutase (SOD), catalase (CAT), pyruvate kinase (PK), and lactate dehydrogenase (LDH). The activities of other metabolic enzymes, phosphofructokinases (PFK), long-chain acyl-CoA dehydrogenase (ACADL), long-chain acyl-CoA synthetase (ACSL), hexokinase (HK), arginase (ARG), glutamate dehydrogenase (GDH), and glutaminase (GLM), were measured using the enzyme-linked immune sorbent assay (ELISA) kit (RapidBio, USA). The assay was performed according to the instructions of the manufacturer, and the detailed assay procedure is shown in Supporting Information (SI). All biochemical determinations were normalized to the protein content.

Metabolism Quenching and Metabolites Extraction. Six replicates were performed for the control and each dose of treatment. When the SCCPs exposure experiment was finished, the culture medium was removed. Cells were rinsed by gently dispensing 2 mL of ultrapure water to the surface, aspirated rapidly within 10 s, and then quenched by liquid nitrogen freezing. Approximately 5 mL of liquid nitrogen was used to completely fill the well. When liquid nitrogen was evaporated off, 2 mL of MeOH was immediately added to each well. Cells were scraped by a cell lifter and transferred to an Eppendorf tube.²⁷ The obtained cells were freeze-dried and stored in a –80 °C freezer for further extraction and analysis.

The extraction of intracellular metabolites was performed according to a method reported by Whiley et al.²⁸ MTBE was used to extract apolar metabolites from HepG2 cells. The Eppendorf tube containing HepG2 cells from each well was added with 400 μL of MTBE and then vortexed for 20 min at room temperature. After the addition of 260 μL of ultrapure water, the sample was mixed and centrifuged for 15 min at 10 000 g, 4 °C. Finally, 200 μL of the upper MTBE phases were transferred to new glass vials, dried with N₂, and reconstituted

in 200 μL of ACN for the analysis of the apolar fractions. Prior to extraction, 10 μL of the internal standards solution (norleucine, undecanoic acid, and nonadecanoic acid in acetonitrile, 10 $\mu\text{g}/\text{L}$) was added as recovery correction for quantitative analysis. Methanol was used to extract the polar metabolites from the remaining part after MTBE extraction. The extraction was conducted using the mixture of 100 μL of MTBE and 130 μL of methanol. The sample was vortexed for 20 min and then centrifuged for 15 min at 10 000 g . A 200- μL aliquot of the lower methanol–water phase was used directly for the analysis of the polar fractions. For the extraction of extracellular metabolites, the culture medium from each well was transferred into a 2-mL sample tube and centrifuged at 6000 g for 10 min. Supernatant (200 μL) was freeze-dried and further extraction and analysis follow the same process with intercellular metabolites.

LC–MS/MS Analysis. Extracts from the HepG2 cells and culture medium were analyzed by an Accela High Speed LC System (Thermo Fisher Scientific, San Jose, CA, USA) equipped with a TSQ Quantum Access MAX triple quadrupole (Thermo Fisher Scientific). The analyses of the polar fraction and apolar fractions were performed in two analytical modes. A C_8 HPLC column (2.1 mm \times 150 mm \times 3 μm) was used for the chromatographic separation of the apolar fraction, with injection volume of 10 μL and total analysis time within 20 min, mobile phase was H_2O , acetonitrile (ACN), and ACN containing 5 mM ammonium acetate; correspondingly, a reverse-phase HPLC C_{18} column (2.1 mm \times 150 mm \times 3 μm ; Waters, Milford, MA, USA) was used for the chromatographic separation of the polar fraction, mobile phase was H_2O containing 0.5% formic acid and methanol, the injection volume was 2 μL and total time taken was 18 min. N_2 was used as the auxiliary gas and sheath gas. The MS was operated in a positive ion mode with dynamic multiple reaction monitoring (MRM) for the detection of the amino acids profiles, lactic acid, urea, and glycerol, whereas negative ion modes with MRM was used for the detection of glucose and free fatty acid profiles. The details on operating parameters of LC–MS/MS are given in Supporting Information (Tables S1 and S2).

Data Processing. Thermo Fisher Xcalibur 2.1 was used for data acquisition and qualitative analysis. Before statistical analysis, the concentration of each detected metabolite across all samples was normalized to the total concentrations of the corresponding samples (sum of all the detected metabolites in one sample) to balance their concentration differences resulted from the discrepancies in the number of cells for each sample. Multivariate analysis was performed using SIMCA-P11.5 software (Umetrics, Sweden). P values of <0.05 were considered as significantly different from the control. Partial least-squares discriminate analysis (PLS-DA) was applied with unit variance (UV) scaling, and hierarchical cluster analysis (HCA) was conducted using MeV software package (version 4.8.1). The metabolite set enrichment analysis and pathway analysis were based on MetaboAnalyst,²⁹ a web service for metabolomics data analysis.

RESULTS AND DISCUSSION

Cell Viability. The HepG2 cells were first incubated with different concentrations of C_{10} -CPs (1, 10, 100 $\mu\text{g}/\text{L}$; Cl, 60.9%) for 24 and 48 h, respectively. As shown in Figure 1A, C_{10} -CPs produced an obvious impairment of cell viability. After 24-h exposure, middle- and high-dose C_{10} -CPs produced statistically significant cell lethality compared with the negative

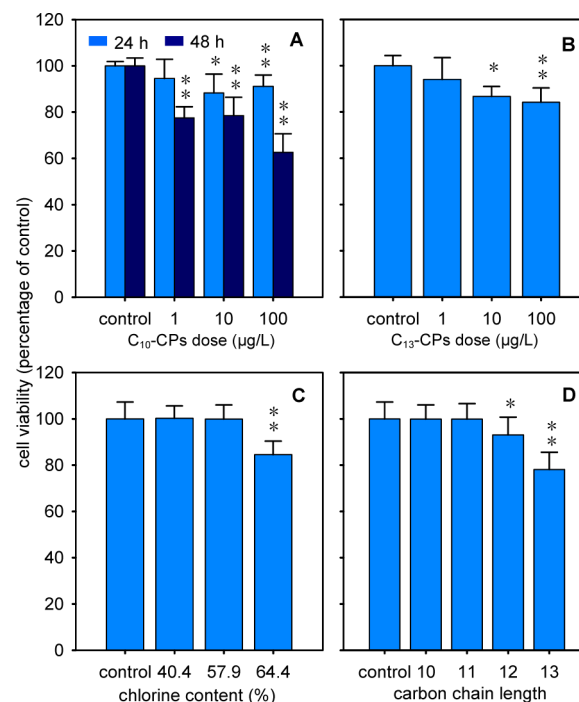


Figure 1. Viability of HepG2 cells exposed to SCCPs. (A) exposure to C_{10} -CPs (Cl, 60.9%) with different concentrations, (B) exposure to C_{13} -CPs (Cl, 55.0%) with different concentrations, (C) exposure to C_{10} -CPs (100 $\mu\text{g}/\text{L}$) with different chlorine contents, (D) exposure to SCCPs (100 $\mu\text{g}/\text{L}$) with the similar chlorine contents (Cl, 55.0%–57.9%) and different carbon chain lengths. Significant differences were indicated in comparison of the control by Student t -test. *, $P < 0.05$; **, $P < 0.01$.

control ($P < 0.05$). Exposure for 48 h with C_{10} -CPs resulted in more reduction in cell viability, showing a significant decrease at all three concentrations of C_{10} -CPs. Moreover, 24-h incubation with different concentrations of C_{13} -CPs (1, 10, 100 $\mu\text{g}/\text{L}$; Cl, 55.0%) clearly indicated a decreasing tendency in cell viability with increasing doses, and a significant effect on cell viability was observed at concentrations of 10 and 100 $\mu\text{g}/\text{L}$ (Figure 1B).

The effects of carbon chain length and chlorine content of SCCPs on HepG2 cell viability were further investigated. Cells were incubated with different SCCPs formulas at the same concentration of 100 $\mu\text{g}/\text{L}$ for 24 h. As shown in Figure 1C, two formulas of C_{10} -CPs with chlorine contents of 40.4% and 57.9% did not exhibit an inhibitory effect on cell viability; only C_{10} -CPs with the highest chlorine content (64.4%) led to a significant decrease of 15% ($P < 0.01$) in cell viability. When HepG2 cells were exposed to SCCPs formulas with the similar chlorine contents (Cl, 55.0%–57.9%), cell viabilities were not significantly altered by C_{10} -CPs and C_{11} -CPs; whereas cells treated with C_{12} -CPs and C_{13} -CPs exhibited significant cytotoxicity, with reductions of 7% and 22% in cell viability, respectively (Figure 1D).

An earlier toxicity study that examined the toxicological mode of action of chlorinated paraffins indicated that C_{10} -CPs induced more severe histopathologies in the liver of juvenile rainbow trout (*Oncorhynchus mykiss*) than did C_{11} -, C_{12} -, and C_{14} -CPs, and the toxicity of SCCPs was inversely related to carbon chain length.³⁰ However, our study suggests that SCCPs with a longer carbon chain and higher chlorine content are prone to producing higher in vitro cytotoxicity. SCCPs with a

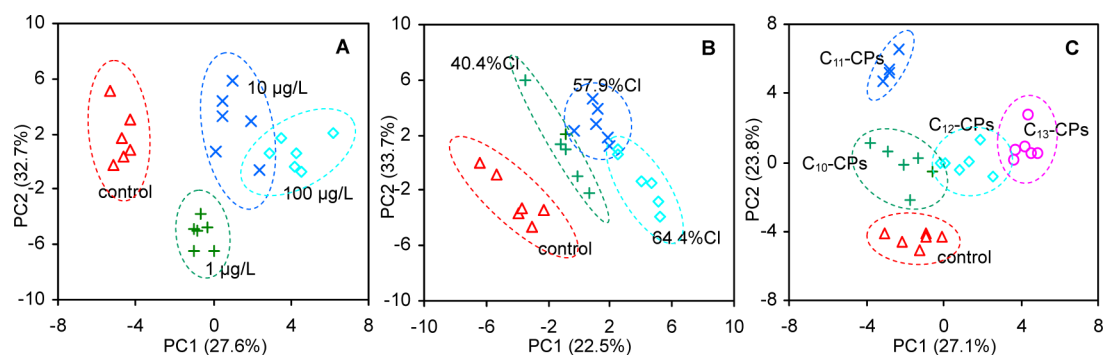


Figure 2. PLS-DA score plots of metabolites in HepG2 cells exposed to (A) C_{13} -CPs (Cl, 60.9%) with different doses, (B) C_{10} -CPs (100 $\mu\text{g/L}$) with different chlorine contents, and (C) SCCPs (100 $\mu\text{g/L}$) with the similar chlorine contents (Cl, 55.0%–57.9%) and different carbon chain lengths.

longer carbon chain and higher chlorine content had a higher octanol–water partition coefficient (K_{OW}).³¹ The increased cytotoxicity induced by SCCPs with higher K_{OW} values might result from their larger partition into HepG2 cells from the culture medium. In a previous *in vitro* cytotoxicity study of chlorinated alkanes, Zvinavashe et al. demonstrated a strong correlation between the acute *in vitro* toxicity of chlorinated alkanes and their $\log K_{OW}$ values in Chinese hamster ovary cells.³²

Oxidative Stress Responses. The loss of cell viability should be mainly resulted from cell energy deficiency and metabolic disorder, all of which can be primarily driven by oxidative stress.³³ To counteract the oxidative stress induced by SCCPs exposure, the antioxidant defense system in HepG2 cells would be inevitably altered. We observed that CAT activity significantly increased with the increase of SCCPs doses from 0 to 100 ng/L, and the SOD activities were slightly higher at middle-dose exposure (10 ng/L) and high-dose exposure (100 ng/L) when compared to the control (Supporting Information Figure S2). Meanwhile, GSH contents in HepG2 cells were significantly decreased after exposure to middle- and high-dose SCCPs. These results clearly indicated a dose-dependent variation of cellular oxidative status.

Metabolic Profiling. The established analytical method for targeted metabolites was applied to profile the metabolic changes in HepG2 cells in response to SCCPs exposure. A total of 43 metabolites were quantified, and most of these metabolites showed significant concentration differences among different treatment settings. A one-way analysis of variance was calculated to test the robust differences among different treatment settings, and the results are showed in Supporting Information Table S4.

For the set of control and dose-dependent groups, 39 out of 43 metabolites were differentially produced ($P < 0.05$), with a false discovery rate (FDR) of < 0.05 . Likewise, for the set of control and chlorine content-dependent groups, 40 metabolites were differentially produced ($P < 0.05$), with an FDR of < 0.05 ; correspondingly, all quantified metabolites showed significant differences for the set of control and carbon chain length-dependent groups. Different SCCPs treatments resulted in more or less different alterations of metabolic profiles in the HepG2 cells. Nevertheless, it was found that all SCCPs treatments induced larger fold changes (FC) in concentrations of adrenic acid ($\log_2\text{FC} > 3.38$) and proline ($\log_2\text{FC} < -0.67$) (Supporting Information Table S5). This result suggests that adrenic acid and proline may serve as two potential biomarkers for the diagnosis of SCCPs exposure.

Glucose and 15 amino acids were supplied as nutrients for HepG2 cell growth in the culture medium. It was found that the concentrations of glucose and 13 amino acid nutrients in extracellular culture medium were slightly decreased after the HepG2 cells were exposed to the low-dose C_{13} -CPs (Supporting Information Figure S3). On the contrary, the intracellular concentrations of glucose and 11 amino acid nutrients in the low-dose group were enhanced slightly compared with the control (Supporting Information Figure S4). These results indicated that exposure to low-dose SCCPs promoted the import of extracellular nutrients into the HepG2 cells.

Multivariate Pattern Recognition Analysis. To further determine the metabolic alterations related to SCCPs intervention, PLS-DA was performed to the normalized data sets for all detected 43 metabolites. The PLS-DA score plots showed that all SCCPs exposure groups were clearly distinct from the control group (Figure 2). Even the low-dose group (1 $\mu\text{g/L}$) exhibited significant metabolic perturbation induced by SCCPs (Figure 2A). The difference between the low-dose and control groups was displayed along the PC2 direction, whereas the high-dose (100 $\mu\text{g/L}$) and middle-dose groups (10 $\mu\text{g/L}$) better separated from the control group along the PC1 direction.

As shown in Figure 2B, SCCPs exposure group with higher chlorine content showed a greater separation from the control group mainly along PC1 direction. This result suggested that SCCPs with higher chlorine content caused more pronounced metabolic perturbation. In the PLS-DA score plot for the data set of the control and carbon chain length-dependent groups (Figure 2C), SCCPs exposure groups showed a clear separation from the control group mainly along PC2 direction, and the different carbon chain length groups also exhibited a separation trend.

Hierarchical Clustering Analysis. To visualize the relationship between these metabolites, hierarchical clustering was used to arrange the metabolites based on their relative levels across groups. Metabolites with significantly altered concentrations ($P < 0.05$) in the data set of control and dose-dependent groups were used for clustering analysis. The normalized data were analyzed based on the Pearson correlation coefficients and visualized in a heat map (Supporting Information Figure S5). Metabolites with a similar dose–response relationship were clearly clustered in the left tree, and four exposure–response trajectories were generated.

In group A, six kinds of amino acids (glutamine, aspartic acid, glycine, alanine, glutamate, and cysteine) together with myristic

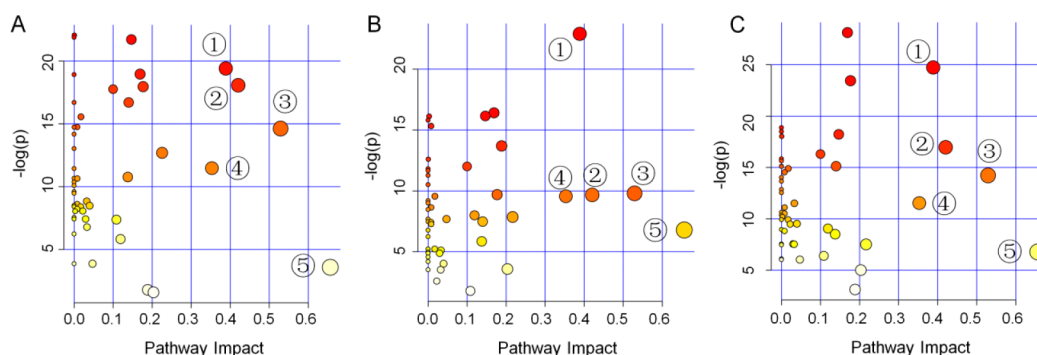


Figure 3. Global metabolic disorders of the most relevant pathways influenced by SCCPs. (A) Pathway influenced after exposure to C_{13} -CPs (Cl, 55.0%) with different concentrations (0, 1, 10, 100 $\mu\text{g/L}$), (B) exposure to C_{10} -CPs (100 $\mu\text{g/L}$) with different chlorine contents (Cl, 40.4%, 57.9%, and 64.4%), (C) exposure to SCCPs (100 $\mu\text{g/L}$) with the similar chlorine contents (Cl, 55.0%–57.9%) and different carbon chain lengths (C_{10} , C_{12} , C_{13}).

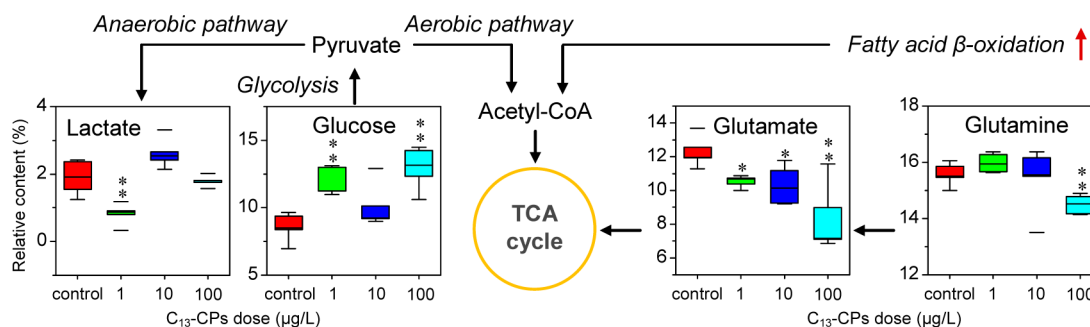


Figure 4. Disturbed pathways of energy metabolism by C_{13} -CPs (Cl, 55.0%) with different exposure doses. Significant differences were indicated in comparison of the control by Student *t*-test. *, $P < 0.05$; **, $P < 0.01$.

acid exhibited a significant decrease in high-dose group compared with the control. Most of unsaturated fatty acids clustered in group B, displaying a decrease in three SCCPs exposure groups compared with the control. On the contrary, most of saturated fatty acids were classified into group C, which presented an obvious elevation in the middle- and high-dose SCCPs exposure groups. Twelve kinds of amino acids together with glucose and urea clustered in group D, exhibiting a rising trend from control to low-dose and then decreased in the middle-dose followed by a rebound in the high-dose groups. These inherent biological variations in metabolite production could at least partially underlie the self-regulation of HepG2 cells after intervention by SCCPs exposure.

Disturbance of Metabolic Pathway. Metabolic pathway perturbation induced by SCCPs intervention was further studied using MetaboAnalyst based on the significantly different metabolites. Pathway analysis was conducted to reveal the most relevant pathways affected by different exposure doses. SCCPs intervention was considered to be highly responsible for the perturbation of arginine and proline metabolism; glycine, serine, and threonine metabolism; alanine, aspartate, and glutamate metabolism; D-glutamine and D-glutamate metabolism; and linoleic acid metabolism (Figure 3). Furthermore, pathway enrichment analysis indicated protein biosynthesis, urea cycle, ammonia recycling and β -oxidation of long chain fatty acids were also disturbed (Supporting Information Figure S6). Metabolic pathways influenced by different chain length and chlorine content were also analyzed. The most relevant perturbed pathways were almost consistent with dosage disruption (Figure 3 and Supporting Information Figure S6). These findings indicated that the underlying toxicity

mechanism of SCCPs in HepG2 cells should be identical after short-term exposure. The detailed information regarding pathway perturbation is discussed as follows using dosage effects.

Perturbation in Energy Metabolism. In oncology, most cancer cells have been observed to predominantly produce energy by a higher rate of glycolysis that converts glucose into pyruvate.^{34,35} In our study, glucose and glutamine were supplied in DMEM culture medium as the major energy sources for HepG2 cell growth. We found that SCCPs intervention induced an obvious fluctuation of glycolysis. As shown in Figure 4, SCCPs intervention obviously altered glucose level in HepG2 cells. Glucose first increased from the control to the low dose, and then decreased in the middle dose, followed by a rebound in the high-dose group.

The main control step of glycolysis is the conversion of fructose-6-phosphate to fructose-1,6-bisphosphate catalyzed by PFK and other two rate-limiting enzymes are HK and PK. The activities of HK, PFK, and PK in HepG2 cells were determined. It was found that PFK activity presented an increasing tendency with the increase of SCCPs exposure dose, and PFK activity was significantly higher in the high-dose exposure group compared with the control (Supporting Information Figure S7). However, SCCPs addition significantly inhibited the activity of HK, and PK activity was also significantly decreased after exposure to the high-dose SCCPs (Supporting Information Figure S7).

Lactate can be produced in anaerobic glycolysis, and LDH catalyzes the conversion of pyruvate to lactate and back. As shown in Figure 4, lactate first significantly decreased from the control to the low dose, and then recovered in the middle dose,

followed by a significant reduction in the high-dose group. The variation trend was exactly opposite to that of glucose level. We further examined the activity of LDH. It was found that the activity of LDH exhibited a significant increase after exposure to SCCPs (Supporting Information Figure S7). The result implied that the anaerobic pathway of glycolysis in HepG2 cells was generally disturbed in the SCCPs exposure groups.

Glutamine as another important carrier of energy was significantly decreased after exposure to the high-dose SCCPs compared with the control. Glutamine can be metabolized into glutamate by the enzyme GLM. We observed that glutamate was significantly reduced after exposure to SCCPs, and its content exhibited a decreasing tendency with increasing SCCPs dose. However, the activity of GLM did not present a significant change after exposure to SCCPs (Supporting Information Figure S7). Furthermore, glutamate can be metabolized into 2-oxoglutarate by the enzyme GDH to enter the TCA cycle for energy production. It was found that the activity of GDH exhibited a rising trend with increasing SCCPs dose (Supporting Information Figure S7). These results clearly showed that SCCPs exposure led to the up-regulation of glutamine metabolism. Therefore, the energy production from glutamine metabolism would be enhanced.

The β -oxidation of fatty acids is also an important energy production pathway by which fatty acid molecules broken down to generate acetyl-coA. In this study, SCCPs exposure caused a decrease in most unsaturated fatty acids and long-chain fatty acids in the HepG2 cells, especially in the high-dose group. Meanwhile, two kinds of short-chain fatty acids hexanoic acid and octanoic acid presented a significant increase after exposure to middle- and high-dose SCCPs. We further examined the activities of ACADL and ACSL. They both exhibited an increasing tendency with increasing SCCPs dose, and the activities of ACADL and ACSL were both significantly higher in the middle- and high-dose groups compared with the control (Supporting Information Figure S7). These results clearly indicated that SCCPs exposure generally accelerated the β -oxidation of fatty acids. The up-regulation of fatty acid β -oxidation would stimulate the consumption of fatty acids as energy to partly compensate for the decrease in energy production from the glucose and glutamine metabolism. The β -oxidation of fatty acids can occur in peroxisomes, especially the long-chain fatty acids. The β -oxidation should result from peroxisome proliferation in HepG2 cells. A previous toxicology study has reported hepatic peroxisome proliferation in male rats and mice exposed to SCCPs.³⁶ The consumption of fatty acids evidently induced the depletion of lipids in HepG2 cells. The lipid depletion phenomenon has been observed in the livers of juvenile rainbow trout (*Oncorhynchus mykiss*) exposed to high dietary concentrations of SCCPs.³⁰

Perturbation in Amino Acid Metabolism. Amino acids are the building blocks of proteins and have many functions in the body. In this study, SCCPs exposure induced a significant disorder of amino acid metabolism in HepG2 cells (Supporting Information Figure S8). The most relevant metabolic pathway of amino acids affected by SCCPs exposure included glycine, serine, and threonine metabolism; arginine, and proline metabolism; alanine, aspartate, and glutamate metabolism; and glutamine and glutamate metabolism (Figure 3). In the metabolic pathway of glycine, serine, and threonine, the contents of serine and threonine in HepG2 cells both presented a significant increase from the control to the low dose, followed by a sharp decline in middle and high doses, whereas glycine

exhibited a continuous decrease from the control to high dose. This result implied that exposure to middle- and high-dose SCCPs could inhibit the glycine, serine, and threonine metabolism in HepG2 cells. Serine and glycine are essential precursors for the biosynthesis of glutathione, purines, and lipid head groups. In addition, metabolites of serine are critical for nucleotide synthesis.³⁷

Arginine has multiple metabolic fates and thus is one of the most versatile amino acids. It is metabolically interconvertible with the amino acid proline. In this study, SCCPs exposure caused a significant reduction in proline content. However, arginine content was first down-regulated at the low dose of SCCPs, and then sharply rebounded at the middle and high doses of SCCPs.

As shown in Figure 4, glutamate was almost linearly decreased with increasing SCCPs dose. Glutamate is an important excitatory neurotransmitter and used as an intercellular signaling molecule.³⁸ The significant decrease of glutamate may result in a disorder of intercellular communication. A previous study also demonstrated that SCCPs may act as tumor promoters for the inhibition of rat liver gap junction intercellular communication.³⁹ Similar to glutamate, significant decreases in alanine induced by SCCPs exposure were also observed. Alanine production is an important indicator for ammonia detoxification. Down-regulation of alanine implied the possible accumulation of ammonia in the cells.

Perturbation in the Urea Cycle. The urea cycle is a cycle of biochemical reactions that remove ammonia (NH_3) by converting it into the relatively nontoxic urea. Ammonia comes from oxidative deamination of the amino acid. As described above, low-dose SCCPs promoted the import of amino acids from culture medium into the cells (Supporting Information Figures S3 and S4). However, the extracellular and intracellular concentrations of arginine were both significantly decreased in the low-dose group compared with the control. The significant decrease was simultaneously accompanied by the up-regulation of urea and ornithine (Figure 5). These results clearly indicated that the urea cycle was up-regulated after exposure to low-dose SCCPs and thus ammonia detoxification would be accelerated.

The intracellular concentrations of glutamine, aspartate, arginine, ornithine, and urea in the middle-dose SCCPs exposure group were all comparable with those in the control group. However, when HepG2 cells were exposed to high-dose SCCPs, the contents of glutamine, glutamate, and aspartate were significantly decreased compared with the control. On the contrary, arginine presented a significant increase, and urea content also showed a rebound. We further examined the activity of enzyme ARG, which catalyze the conversion of arginine into urea and ornithine. It was found that the activity of ARG was significantly higher in the high-dose exposure group compared with the control (Supporting Information Figure S7). These results suggested that high-dose SCCPs exposure also led to the up-regulation of urea cycle.

Some Insights into Toxicity Mechanism. Our data suggest that exposure to environmental dose-related SCCPs produce a significant toxic effect on HepG2 cells, which is comprehensively reflected by the reduction in the cell viability, alteration in the intracellular redox status and disturbance in the metabolite profile. On the basis of previous studies and our results, the possible mechanisms of SCCPs toxicity are deduced as follows. First, as a kind of chloro-alkane SCCPs act as a peroxisome proliferator to induce the peroxisome proliferation,⁴⁰ and therefore, the β -oxidation of unsaturated fatty acids

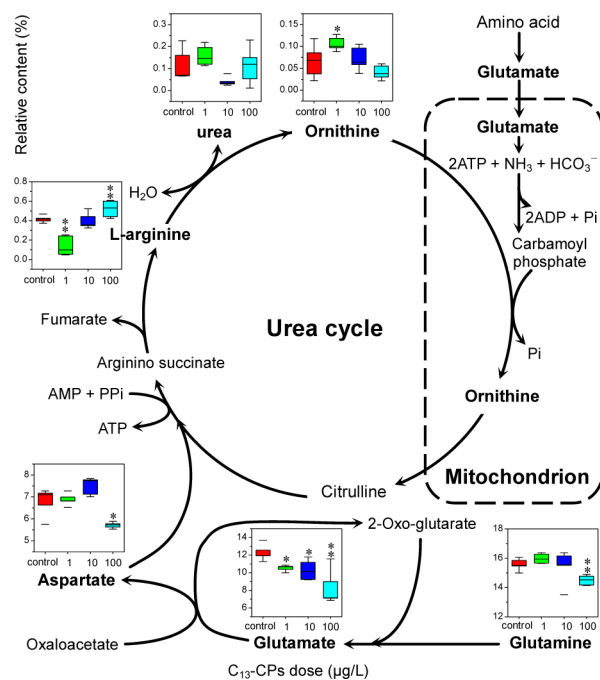


Figure 5. Disturbance of urea cycle after exposure to C₁₃-CPs (Cl, 55.0%) with different doses. Significant differences were indicated in comparison of the control by Student *t*-test. *, *P* < 0.05; **, *P* < 0.01.

and long-chain fatty acids was specifically accelerated.⁴¹ Second, as a kind of xenobiotics SCCPs are inevitably metabolized by cytochrome P450 enzymes and therefore lead to the oxidative stress;^{42,43} as the adaptive responses to oxidative stress, energy metabolism and amino acid metabolism are disturbed, and urea cycle is up-regulated. Finally, cell lipids are excessively consumed because of the up-regulation of fatty acid β -oxidation, and protein biosynthesis are inhibited due to the disturbance in amino acid metabolism. The induced oxidative stress, excessive consumption of lipids, and inhibition of protein biosynthesis should be jointly responsible for the reduction in cell viability. To make sure the mode of action induced by SCCPs, genomic and proteomic evidence on SCCPs toxicity should be further provided.

■ ASSOCIATED CONTENT

📄 Supporting Information

Detailed description on LC-MS/MS analysis, QA/QC and ELISA procedure, ANOVA results and fold changes for differential metabolites, results of metabolic pathway enrichment analysis, SCCPs-induced perturbation of extracellular and intracellular nutrients, effects of SCCPs exposure on several oxidative stress markers and relevant metabolic enzyme activities, disturbed pathways of amino acid metabolism in citric acid cycle. This material is available free of charge via the Internet at <http://pubs.acs.org>.

■ AUTHOR INFORMATION

Corresponding Authors

*Phone: +86-411-8437-9972. Fax: +86-411-8437-9562. E-mail: hjzhang@dicp.ac.cn.

*Phone/fax: +86-411-8437-9562. E-mail: chenjp@dicp.ac.cn.

Notes

The authors declare no competing financial interest.

■ ACKNOWLEDGMENTS

The authors thank the National Natural Science Foundation of China (Grants 21277141 and 21337002) and the National High-Tech R&D Plan (863 Program: 2013AA065203) for financial support.

■ REFERENCES

- (1) Ali, T. S.; Legler, J. Overview of the mammalian and environmental toxicity of chlorinated paraffins. In *Chlorinated Paraffins*; Boer, J., Ed.; Springer: Berlin, 2010; pp 135–154.
- (2) Barber, J. L.; Sweetman, A. J.; Thomas, G. O.; Braekvelt, E.; Stern, G. A.; Jones, K. C. Spatial and temporal variability in air concentrations of short-chain (C₁₀–C₁₃) and medium-chain (C₁₄–C₁₇) chlorinated *n*-alkanes measured in the U.K. atmosphere. *Environ. Sci. Technol.* **2005**, *39* (12), 4407–4415 DOI: 10.1021/es047949w.
- (3) Gao, Y.; Zhang, H. J.; Su, F.; Tian, Y. Z.; Chen, J. P. Environmental occurrence and distribution of short chain chlorinated paraffins in sediments and soils from the Liaohe River Basin, P. R. China. *Environ. Sci. Technol.* **2012**, *46* (7), 3771–3778 DOI: 10.1021/es2041256.
- (4) Yuan, B.; Wang, T.; Zhu, N. L.; Zhang, K. G.; Zeng, L. X.; Fu, J. J.; Wang, Y. W.; Jiang, G. B. Short chain chlorinated paraffins in Mollusks from coastal waters in the Chinese Bohai Sea. *Environ. Sci. Technol.* **2012**, *46* (12), 6489–6496 DOI: 10.1021/es203839h.
- (5) Zeng, L. X.; Wang, T.; Han, W. Y.; Yuan, B.; Liu, Q. A.; Wang, Y. W.; Jiang, G. B. Spatial and vertical distribution of short chain chlorinated paraffins in soils from wastewater irrigated farmlands. *Environ. Sci. Technol.* **2011**, *45* (6), 2100–2106 DOI: 10.1021/es103740v.
- (6) Tomy, G. T.; Stern, G. A.; Lockhart, W. L.; Muir, D. C. G. Occurrence of C₁₀–C₁₃ polychlorinated-*n*-alkanes in Canadian Midlatitude and Arctic Lake sediments. *Environ. Sci. Technol.* **1999**, *33* (17), 2858–2863 DOI: 10.1021/es990107q.
- (7) Bezchlebová, J.; Černohlávková, J.; Kobetičová, K.; Lána, J.; Sochová, I.; Hofman, J. Effects of short-chain chlorinated paraffins on soil organisms. *Ecotoxicol. Environ. Safe.* **2007**, *67* (2), 206–211 DOI: 10.1016/j.ecoenv.2006.12.015.
- (8) Tomy, G. T.; Muir, D. C. G.; Stern, G. A.; Westmore, J. B. Levels of C₁₀–C₁₃ polychloro-*n*-alkanes in marine mammals from the Arctic and the St. Lawrence River Estuary. *Environ. Sci. Technol.* **2000**, *34* (9), 1615–1619 DOI: 10.1021/es990976f.
- (9) Wang, T.; Wang, Y. W.; Jiang, G. B. On the environmental health effects and socio-economic considerations of the potential listing of short-chain chlorinated paraffins into the Stockholm Convention on Persistent Organic Pollutants. *Environ. Sci. Technol.* **2013**, *47* (21), 11924–11925 DOI: 10.1021/es403705n.
- (10) Revised draft risk profile: short-chained chlorinated paraffins, UNEP/POPS/POPRC.6/11/Rev.1, Stockholm Convention on Persistent Organic Pollutants, Geneva, 2011.
- (11) Bucher, J. R.; Alison, R. H.; Montgomery, C. A.; Huff, J.; Haseman, J. K.; Farnell, D.; Thompson, R.; Prejean, J. D. Comparative toxicity and carcinogenicity of two chlorinated paraffins in F344/N rats and B6C3F1 mice. *Fundam. Appl. Toxicol.* **1987**, *9* (3), 454–468 DOI: 10.1016/0272-0590(87)90028-5.
- (12) Nielsen, E.; Ladefoged, O. *Evaluation of Health Hazards by Exposure to Chlorinated Paraffins and Proposal of a Health-Based Quality Criterion for Ambient Air*; The Danish Environmental Protection Agency: Copenhagen, 2013; p 38–39.
- (13) Leon, Z.; Garcia-Canaveras, J. C.; Donato, M. T.; Lahoz, A. Mammalian cell metabolomics: Experimental design and sample preparation. *Electrophoresis* **2013**, *34* (19), 2762–2775 DOI: 10.1002/elps.201200605.
- (14) Griffin, J.; Bollard, M. Metabonomics: Its potential as a tool in toxicology for safety assessment and data integration. *Curr. Drug Metab.* **2004**, *5* (5), 389–398 DOI: 10.2174/1389200043335432.
- (15) Sreekumar, A.; Poisson, L. M.; Rajendiran, T. M.; Khan, A. P.; Cao, Q.; Yu, J.; Laxman, B.; Mehra, R.; Lonigro, R. J.; Li, Y.; Nyati, M. K.; Ahsan, A.; Kalyana-Sundaram, S.; Han, B.; Cao, X.; Byun, J. J.

Omenn, G. S.; Ghosh, D.; Pennathur, S.; Alexander, D. C.; Berger, A.; Shuster, J. R.; Wei, J. T.; Varambally, S.; Beecher, C.; Chinnaiyan, A. M. Metabolomic profiles delineate potential role for sarcosine in prostate cancer progression. *Nature* **2009**, *457* (7231), 910–914 DOI: 10.1038/nature07762.

(16) O’Kane, A. A.; Chevignier, O. P.; Graham, S. F.; Elliott, C. T.; Mooney, M. H. Metabolomic profiling of *in vivo* plasma responses to dioxin-associated dietary contaminant exposure in rats: Implications for identification of sources of animal and human exposure. *Environ. Sci. Technol.* **2013**, *47* (10), 5409–5418 DOI: 10.1021/es305345u.

(17) Jones, O. A.; Spurgeon, D. J.; Svendsen, C.; Griffin, J. L. A metabolomics based approach to assessing the toxicity of the polyaromatic hydrocarbon pyrene to the earthworm *Lumbricus rubellus*. *Chemosphere* **2008**, *71* (3), 601–609 DOI: 10.1016/j.chemosphere.2007.08.056.

(18) Ji, C. L.; Wu, H. F.; Wei, L.; Zhao, J. M.; Lu, H. J.; Yu, J. B. Proteomic and metabolomic analysis of earthworm *Eisenia fetida* exposed to different concentrations of 2,2',4,4'-tetrabromodiphenyl ether. *J. Proteomics* **2013**, *91*, 405–416 DOI: 10.1016/j.jprot.2013.08.004.

(19) Lankadurai, B. P.; Simpson, A. J.; Simpson, M. J. H-1 NMR metabolomics of *Eisenia fetida* responses after sub-lethal exposure to perfluorooctanoic acid and perfluorooctane sulfonate. *Environ. Chem.* **2012**, *9* (6), 502–511 DOI: 10.1071/EN12112.

(20) Zeng, J.; Kuang, H.; Hu, C. X.; Shi, X. Z.; Yan, M.; Xu, L. G.; Wang, L. B.; Xu, C. L.; Xu, G. W. Effect of bisphenol A on rat metabolic profiling studied by using capillary electrophoresis time-of-flight mass spectrometry. *Environ. Sci. Technol.* **2013**, *47* (13), 7457–7465 DOI: 10.1021/es400490f.

(21) Iyer, V. V.; Yang, H.; Ierapetritou, M. G.; Roth, C. M. Effects of glucose and insulin on HepG2-C3A cell metabolism. *Biotechnol. Bioeng.* **2010**, *107* (2), 347–356 DOI: 10.1002/bit.22799.

(22) Hockley, S. L.; Mathijs, K.; Staal, Y. C.; Brewer, D.; Giddings, L.; van Delft, J. H.; Phillips, D. H. Interlaboratory and interplatform comparison of microarray gene expression analysis of HepG2 cells exposed to benzo(a)pyrene. *Omic* **2009**, *13* (2), 115–125 DOI: 10.1089/omi.2008.0060.

(23) Bai, J.; Wang, M. X.; Chowbay, B.; Ching, C. B.; Chen, W. N. Metabolic profiling of HepG2 cells incubated with S(-) and R(+) enantiomers of anti-coagulating drug warfarin. *Metabolomics* **2011**, *7* (3), 353–362 DOI: 10.1007/s11306-010-0262-3.

(24) Bayen, S.; Obbard, J. P.; Thomas, G. O. Chlorinated paraffins: A review of analysis and environmental occurrence. *Environ. Int.* **2006**, *32*, 915–929 DOI: 10.1016/j.envint.2006.05.009.

(25) Thomas, G. O.; Farrar, D.; Braekevelt, E.; Stern, G.; Kalantzi, O. I.; Martin, F. L.; Jones, K. C. Short and medium chain length chlorinated paraffins in UK human milk fat. *Environ. Int.* **2006**, *32*, 34–40 DOI: 10.1016/j.envint.2005.04.006.

(26) Tomy, G. T.; Billeck, B.; Stern, G. A. Synthesis, isolation and purification of C₁₀–C₁₃ polychloro-*n*-alkanes for use as standards in environmental analysis. *Chemosphere* **2000**, *40*, 679–683 DOI: 10.1016/S0045-6535(99)00433-6.

(27) Lorenz, M. A.; Burant, C. F.; Kennedy, R. T. Reducing time and increasing sensitivity in sample preparation for adherent mammalian cell metabolomics. *Anal. Chem.* **2011**, *83* (9), 3406–3414 DOI: 10.1021/ac103313x.

(28) Whiley, L.; Godzien, J.; Ruperez, F. J.; Legido-Quigley, C.; Barbas, C. In-vial dual extraction for direct LC-MS analysis of plasma for comprehensive and highly reproducible metabolic fingerprinting. *Anal. Chem.* **2012**, *84* (14), 5992–5999 DOI: 10.1021/ac300716u.

(29) Xia, J. G.; Wishart, D. S. Web-based inference of biological patterns, functions and pathways from metabolomic data using MetaboAnalyst. *Nat. Protoc.* **2011**, *6* (6), 743–760 DOI: 10.1038/nprot.2011.319.

(30) Cooley, H. M.; Fisk, A. T.; Wiens, S. C.; Tomy, G. T.; Evans, R. E.; Muir, D. C. G. Examination of the behavior and liver and thyroid histology of juvenile rainbow trout (*Oncorhynchus mykiss*) exposed to high dietary concentrations of C₁₀, C₁₁, C₁₂ and C₁₄-polychlorinated

n-alkanes. *Aquat. Toxicol.* **2001**, *54* (1–2), 81–99 DOI: 10.1016/S0166-445X(00)00172-7.

(31) Glüge, J.; Bogdal, C.; Scheringer, M.; Buser, A. M.; Hungerbühler, K. Calculation of physicochemical properties for short- and medium-chain chlorinated paraffins. *J. Phys. Chem. Ref. Data.* **2013**, *42* (2), No. 023103, DOI: 10.1063/1.4802693.

(32) Zvinavashe, E.; van den Berg, H.; Soffers, A. E. M. F.; Vervoort, J.; Freidig, A.; Murk, A. J.; Rietjens, I. M. C. M. QSAR models for predicting *in vivo* aquatic toxicity of chlorinated alkanes to fish. *Chem. Res. Toxicol.* **2008**, *21* (3), 739–745 DOI: 10.1021/tx700367c.

(33) Tang, S. F.; Yang, L.; Tang, X.; Liu, M. R. The role of oxidized ATM in the regulation of oxidative stress-induced energy metabolism reprogramming of CAFs. *Cancer Lett.* **2014**, *353* (2), 133–144 DOI: 10.1016/j.canlet.2014.07.028.

(34) Gatenby, R. A.; Gillies, R. J. Why do cancers have high aerobic glycolysis? *Nat. Rev. Cancer* **2004**, *4* (11), 891–899 DOI: 10.1038/nrc1478.

(35) Alfaraouk, K. O.; Muddathir, A. K.; Shayoub, M. E. Tumor acidity as evolutionary spite. *Cancers* **2011**, *3* (1), 408–414 DOI: 10.3390/cancers3010408.

(36) Wyatt, I.; Coutss, C. T.; Elcombe, C. R. The effect of chlorinated paraffins on hepatic enzymes and thyroid hormones. *Toxicology* **1993**, *77* (1–2), 81–90 DOI: 10.1016/0300-483X(93)90139-J.

(37) Vacanti, N. M.; Metallo, C. M. Exploring metabolic pathways that contribute to the stem cell phenotype. *Biochim. Biophys. Acta* **2013**, *1830* (2), 2361–2369 DOI: 10.1016/j.bbagen.2012.08.007.

(38) Sharma, M. K.; Seidlitz, E. P.; Singh, G. Cancer cells release glutamate via the cystine/glutamate antiporter. *Biochem. Biophys. Res. Commun.* **2010**, *391* (1), 91–95 DOI: 10.1016/j.bbrc.2009.10.168.

(39) Kato, Y.; Kenne, K. Inhibition of cell-cell communication by commercial chlorinated paraffins in rat liver epithelial IAR 20 cells. *Pharmacol. Toxicol.* **1996**, *79* (1), 23–28 DOI: 10.1111/j.1600-0773.1996.tb00236.x.

(40) Warnasuriya, G. D.; Elcombe, B. M.; Foster, J. R.; Elcombe, C. R. A mechanism for the induction of renal tumours in male Fischer 344 rats by short-chain chlorinated paraffins. *Arch. Toxicol.* **2010**, *84* (3), 233–243 DOI: 10.1007/s00204-009-0489-9.

(41) Vamecq, J.; Cherkaoui-Malki, M.; Andreoletti, P.; Latruffe, N. The human peroxisome in health and disease: The story of an oddity becoming a vital organelle. *Biochimie* **2014**, *98*, 4–15 DOI: 10.1016/j.biochi.2013.09.019.

(42) Brunstrom, B. Effects of chlorinated paraffins on liver weight, cytochrome P-450 concentration and microsomal enzyme activities in chick embryos. *Arch. Toxicol.* **1985**, *57* (1), 69–71 DOI: 10.1007/BF00286579.

(43) Darnerud, P. O. Chlorinated paraffins: Effect of some microsomal-enzyme inducers and inhibitors on the degradation of 1-¹⁴C-chlorododecanes to ¹⁴CO₂ in mice. *Acta. Pharmacol. Toxicol.* **1984**, *55* (2), 110–115 DOI: 10.1111/j.1600-0773.1984.tb01971.x.